dure is based, may depend on the quality of the sample surface.

Finally we would like to point out some consequences of the preceding results for the interpretation of two-photon experiments. In calculations of the polarization dependence of excitonic two-photon absorption,[13] it has been assumed that the exciton states reached in the process transform according to the irreducible representations of the point group of the crystal. This has to be altered in the case of two-photon transitions which are also one-photon active. From the foregoing it is evident that these states should be classified according to the group of the polariton wave vector K, and the polariton should be regarded as the final state of the transition. Because the degeneracy between longitudinal and transverse states is lifted, a more complicated angular dependence of the two-photon absorption should result. These features will be demonstrated in a forthcoming paper.

We would like to acknowledge discussions with G. Güttler, Professor W. Martienssen, Professor J. Treusch, and C. Uihlein. We thank Dr. W. Staude for providing his data prior to publication and Dr. E. Schönherr for supplying high quality CuCl crystals.

---

†Work supported by the Deutsche Forschungsgemeinschaft. Project of the Sonderforschungsbereich "Festkörperspektroskopie" Darmstadt, Frankfurt am Main, Germany.

*Present address: Institut für Physik, Universität Dortmund, Dortmund, Germany.

[1]R. S. Knox, *Theory of Excitons* (Academic, New York, 1963), p. 103 ff.

[2]U. Fano. Phys. Rev. 103, 1202 (1956); J. J. Hopfield, Phys. Rev. 112, 1555 (1958).

[3]J. J. Hopfield, J. Phys. Soc. Jap. Suppl. 21, 77 (1966).

[4]J. J. Hopfield and D. G. Thomas, Phys. Rev. Lett. 15, 22 (1965); C. H. Henry, Phys. Rev. 143, 627 (1966).

[5]C. H. Henry and J. J. Hopfield, Phys. Rev. Lett. 15, 964 (1965).

[6]*Light Scattering Spectra of Solids,* edited by G. B. Wright (Springer, New York, 1969), Sect. A.

[7]S. Nikitine, in *Progress in Semiconductors,* edited by A. F. Gibson, R. E. Burgess, and P. A. Aigrain (Wiley, New York, 1962), Vol. 6, p. 288 ff; M. Cardona, Phys. Rev. 129, 69 (1963).

[8]B. Staginnus, D. Fröhlich, and T. Caps. Rev. Sci. Instrum. 39, 1129 (1968).

[9]Y. Kaifu and T. Komatsu, J. Phys. Soc. Jap. 25, 644 (1968).

[10]K. S. Song, in *Localized Excitations in Solids,* edited by R. F. Wallis (Plenum, New York, 1968), p. 287.

[11]W. Staude, to be published.

[12]We have shifted the energy scale of Staude's reflectivity data (Ref. 11) by about 10^{-3} eV to produce coincidence of the longitudinal branch with our experimental points. Solving the dispersion equation we have only used the real part of ϵ. We have estimated that in the region of interest the imaginary part causes only small corrections which can be neglected within the present accuracy.

[13]M. Inoue and Y. Toyozawa, J. Phys. Soc. Jap. 20, 363 (1965); T. R. Bader and A. Gold, Phys. Rev. 171, 997 (1968).

Quantum Interference of Electron Waves in a Normal Metal*

R. W. Stark† and C. B. Friedberg‡

Department of Physics, University of Arizona, Tucson, Arizona 85721, and Department of Physics and The James Franck Institute, University of Chicago, Chicago, Illinois 60637

(Received 26 January 1971)

Using a very pure single crystal of magnesium we have observed large-amplitude oscillations in the transverse magnetoresistance which result from the direct interference of normal-state electron waves. The amplitudes of these interference oscillations appear to be independent of the kT broadening of the Fermi distribution. The primary result of our experiment shows that these waves are phase coherent at 1.2°K over macroscopic distances of at least 0.01 mm; this corresponds to a quasiparticle lifetime of at least 2×10^{-11} sec.

In our study of the transverse magnetoresistance of magnesium we have observed large-amplitude oscillations resulting from the direct interference of electron waves. Unlike the de Haas-van Alphen and de Haas-Shubnikov oscillations, which are consequences of the phase coherence and quantization of electron states on closed paths, these oscillations are due to the quantum interference of electrons on different branches of an open trajectory. The effect we have observed is the physical equivalent of the Mercereau experiment,[1] in which the interference is generated between phase-coherent superconducting states. In our experiment, however, the phase coherence is in the normal state and is preserved over macroscopic distances *without the benefit of an energy gap.*

The Mercereau interferometer consists of superconducting paths which interact through points of weak coupling provided by thin oxide layers. In our normal-state interferometer, it is the crystal itself which, in the presence of a magnetic field, determines the electron trajectories, or the "geometry" of the interferometer. The crystal also furnishes the points of weak coupling by means of magnetic-field–induced tunneling across the small energy gaps[3] separating path segments of the trajectories.

Figure 1 shows the transverse magnetoresistivity of a magnesium single crystal as a function of magnetic field strength H for a special case in which the magnetoresistivity is dominated by a tiny group of electrons consistuting only about 10^{-4} of the total electron density of states. The three pertinent features of this curve are (1) the monotonically increasing background resistance upon which are superimposed (2) large-amplitude, low-frequency oscillations and (3) smaller-amplitude, high-frequency oscillations, both of which are periodic in H^{-1}. Normally we would interpret all such oscillatory behavior as the direct result of magnetic quantization of the density of states *à la* Onsager.[3] The thermal broadening of the Fermi distribution function

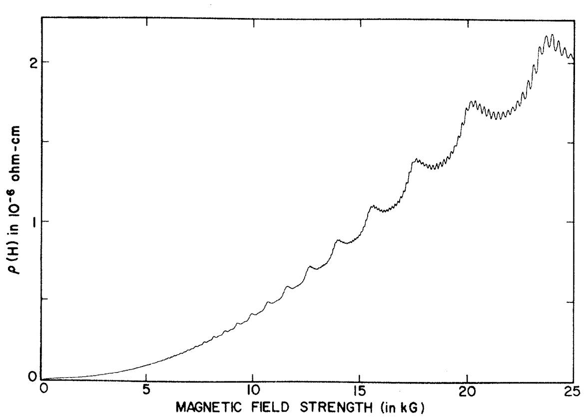

FIG. 1. Transverse magnetoresistivity $\rho(H)$ of a magnesium single crystal at 1.2°K for $\vec{H}$ along a $[10\bar{1}0]$-type crystal axis and the current $\vec{J}$ along a $[11\bar{2}0]$-type axis. Both the monotonic background magnetoresistivity and the large-amplitude, low-frequency oscillations are insensitive to variations in temperature up to 4.2°K. The small-amplitude, high-frequency oscillations vary with temperature, decreasing by a factor of 15 in going to 4.2°K where they are barely visible.

leads directly to a predictable temperature dependence for the amplitude[4] of such oscillations since the resolution of the quantized energy levels depends upon the ratio of the energy-level separation to kT. All previous experiments on the temperature dependence of the amplitude of the de Haas–van Alphen–like phenomena have agreed with the predictions of theory, as do the high-frequency oscillations shown in Fig. 1. In contrast, *the amplitude of the low-frequency oscillations is manifestly insensitive to variations in T* over the range of temperature used in our experiment (1.2-4.2°K). This fact implies that these oscillations do not result from quantized Landau levels or, equivalently, from quantized closed orbits. Fortunately, our knowledge of the electron states in magnesium[5] is detailed enough to allow us to eliminate the possibility of a quantized closed orbit; the frequency in H of the smallest closed orbit is more than one order of magnitude larger than the observed frequency. Furthermore, the interpretation that these oscillations result strictly from interference is not only consistent with our prior knowledge of the electron states, but also, in fact, the details of the effect could have been predicted quantitatively.

Our experiment only measures effects due to electron states on the Fermi surface. Figure 2(a) shows the portions of the Brillouin zone and Fermi surface that are pertinent to our discussion (see Ref. 5 for more detail). The locus of those states with wave vector $\vec{k}$ which are involved in the interference is shown by the darker lines. There are three relevant facts to be considered:

(1) The electrons respond to an applied magnetic field $\vec{H}$ in accord with the Lorentz-force equation

$$\hbar\dot{\vec{k}} = \frac{e}{c}\dot{\vec{r}} \times \vec{H}, \qquad (1)$$

where $\dot{\vec{r}}$ is the group velocity of the electron wave packet in real space. Thus, the trajectory in $\vec{k}$ space occurs with constant energy, for our purposes the Fermi energy, and is mirrored by an identical trajectory in real space scaled by the factor $\hbar c/eH$ and rotated by $\pi/2$ about $\vec{H}$.

(2) Any electron that moves under the influence of $\vec{H}$ from point 1 to point 6 is on an open trajectory,[6] which pumps current along the axis of our crystal in real space, and in so doing totally dominates the magnetoconductivity.

(3) In a finite magnetic field, the probability that an electron will traverse from "1" to "6"

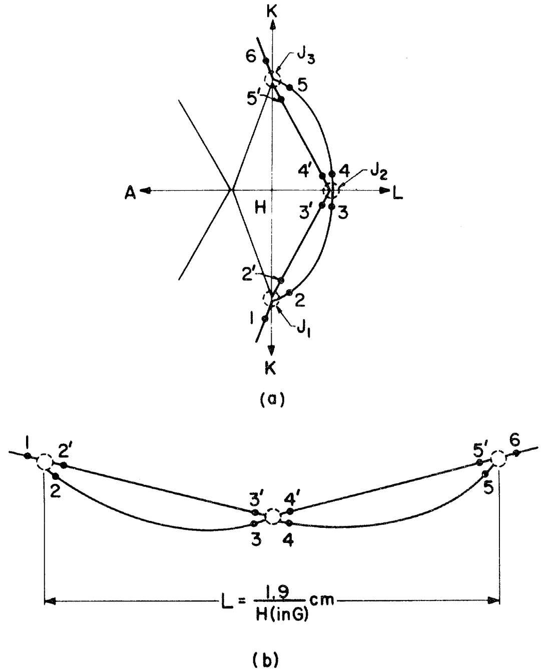

FIG. 2. (a) A cross section of the Brillouin zone and Fermi surface for magnesium (not to scale). The letters A, K, K, H, and L designate symmetry points of the zone. (b) The real space-orbit segments that make up the interferometer; the weak links occur at crystal Bragg-reflection planes.

($|\langle 6|1\rangle|^2$) is less than unity because of the presence of the three junctions J_1, J_2, and J_3 at which there are finite probabilities of interband transitions via magnetic breakdown.[2] J_1 and J_3 are equivalent junctions specified by the same transition probability p_1, but these are not equivalent to J_2 which is specified by a different probability p_2. The transition probabilities for the various paths are

$$|\langle 2'|1\rangle|^2 = |\langle 6|5'\rangle|^2 = p_1^{\,2} = \exp(-H_1/H),$$
$$|\langle 2|1\rangle|^2 = |\langle 6|5\rangle|^2 = 1 - p_1^{\,2},$$
$$|\langle 4|3'\rangle|^2 = |\langle 4'|3\rangle|^2 = p_2^{\,2} = \exp(-H_2/H),$$
$$|\langle 4|3\rangle|^2 = |\langle 4'|3'\rangle|^2 = 1 - p_2^{\,2}, \qquad (2)$$

where we have also indicated the dependence of these on the magnetic field. H_1 and H_2 are constants characterizing the junctions.

The equivalent trajectory segments which make up our "interferometer" in real space are shown in Fig. 2(b). The points designated correspond to the same points in Fig. 2(a). To calculate $|\langle 6|1\rangle|^2$, one needs the following information about phases.

(1) The transmitted and reflected wave functions, respectively $|t\rangle$ and $|r\rangle$, at a junction must be orthogonal. Thus, if

$$|r\rangle = (1-p)\exp(i\varphi_r)$$

and

$$|t\rangle = p\exp(i\varphi_t),$$

then $(\varphi_t - \varphi_r) = (n+\frac{1}{2})\pi$. We will choose the convention $\varphi_t = 0$ and $\varphi_r = \pi/2$.

(2) There is a phase change along each line segment due to the vector potential $\vec{A}$. This is given by

$$\varphi_{23} = \varphi_{45} = (e/\hbar c)\int_2^3 \vec{A}\cdot d\vec{r},$$

and

$$\varphi_{2'3'} = \varphi_{4'5'} = (e/\hbar c)\int_{2'}^{3'} \vec{A}\cdot d\vec{r}. \qquad (4)$$

An important quantity is the phase difference

$$\theta = \varphi_{23} - \varphi_{2'3'} = (e/\hbar c)H\mathcal{A}, \qquad (5)$$

where $\mathcal{A}$ is the area enclosed by one pair of arms of the interferometer.

Using the above information to evaluate the probability amplitudes we find that the transmission probability through the entire interferometer is

$$|\langle 6|1\rangle|^2 = I_0 + I_1\cos\theta + I_2\cos 2\theta, \qquad (6)$$

where

$$I_0 = (1-p_2)^2(1-p_1)^4 + 4p_2^{\,2}p_1^{\,2}(1-p_1)^2 + (1-p_2)^2 p_1^{\,4},$$
$$I_1 = 4p_1p_2(1-p_1)(1-p_2)[p_1^{\,2} - (1-p_1)^2],$$
$$I_2 = -2(1-p_2)^2(1-p_1)^2 p_1^{\,2}. \qquad (7)$$

I_0 is the noninterference portion of the current through the interferometer which results from the inequality of amplitude on the various paths. I_1 is the portion of the interference current which results from wave transfer across the middle junction, that is, from the primed to the unprimed paths and vice versa, while I_2 is the portion for which the wave does not cross the middle junction. Note that the phase difference θ in Eq. (5) is just 2π times the amount of magnetic flux enclosed within half the total area of the interferometer. *This amount of flux is unrestricted, i.e., unquantized.* The dimensional scale factor, $r = \hbar ck/eH$, shows that the linear dimensions of our interferometer decrease as H^{-1}; the area $\mathcal{A}$ decreases as H^{-2} so that the total flux also decreases as H^{-1}. Thus the periodicity of the interference pattern is proportional to H^{-1} as shown in the data in Fig. 1. The experimental periodicity is 7.3×10^{-6} G^{-1}, which agrees well with the theoretical prediction of 7.7×10^{-6} G^{-1} based on our knowledge of the electron states with wave vector $\vec{k}$.[5] At the lowest field for which we have observed these interference oscillations (~2500 G) the length of the interferometer is nearly 0.01 mm. Thus, phase coherence exists in the normal-state electron wave over *at least this distance.*

Our best estimates (which are subject to some uncertainty) for the constants in Eq. (2) are H_1 = 10 kG and H_2 = 1 kG.[7] With these numbers, at a field of 25 kG, p_1 and p_2 are 0.82 and 0.98, respectively, and I_1 and I_2 are 0.011 and 0.000017, respectively. Hence, at this field strength, little of the second-harmonic 2θ interference should exist relative to the fundamental in both the magnetoconductivity and magnetoresistivity. This agrees well with the experimental data in Fig. 1. Equation (7) shows that the second harmonic increases relative to the fundamental at lower field strengths as is also evident in the data. Using the Pippard effective-path formalism[8] we have calculated the ratio of the contribution to the magnetoconductivity of these interfering electron states to that of all other states on the Fermi surface; our results are within a factor of 3 of the experimental data.

A more detailed quantitative comparison between theory and experiment for all values of H requires both more extensive experimental data and more sophisticated calculations of the magnetoconductivity. Part of this study will be the direct determination of the exact values of H_1 and H_2; this will be of importance not only from the viewpoint of obtaining a quantitative understanding of this interferometer, but also from the viewpoint of quantitatively understanding magnetic breakdown.

Of greater importance, however, is the fact that numerical precision in the comparison of theory and experiment is not essential for the immediate utilization of this electron-wave interferometer. This noteworthy feature results from the presence of the interference junction at the exact center of the interferometer. If the typical distance for which the electron wave maintains coherence is λ, then the probability that coherence will be preserved for a distance L is $\exp(-L/\lambda)$. The intensity I_1 requires phase coherence only between adjacent junctions (a distance $L/2$), whereas the intensity I_2 requires phase coherence over twice this distance, i.e., over the entire length L of the interferometer. Thus, for a given H, the experimental ratio $I_1:I_2 = F(H)\exp(-L/\lambda)$, where $F(H)$ can be determined experimentally under conditions for which $\lambda \gg L$. As reported above $\lambda \geq 0.01$ mm for these high purity crystals. If effective scattering perturbations which decrease λ are introduced into the crystal, this decrease may be directly observed in the ratio $I_1:I_2$. Most future work will be directed along these lines. For example, an investigation of the coherent interference-amplitude ratio as a function of temperature will yield information about the electron-phonon interaction; likewise, the introduction of controlled impurity concentrations will yield information about the quasiparticle-impurity scattering cross sections.

Our current bound, $\lambda \geq 0.01$ mm, can be converted into an equivalent bound for the lifetime of the electron quasiparticle by invoking our detailed knowledge of the band structure of magnesium. Integrating electron velocities along orbit segments, we find that it requires 1.86 $\times10^{-11}$ sec for a quasiparticle to traverse an interferometer of length $L = 0.01$ mm. Although at 1.2°K in magnesium with an impurity concentration of about one part in 10^8 the electron-quasiparticle lifetime may be limited by phonon or impurity scattering, the electron-electron scattering lifetime is no smaller than 2×10^{-11} sec.

---

*Work supported in part by National Science Foundation and U. S. Army Research Office (Durham) grants to the University of Chicago, and a National Science Foundation Science Development Grant to the University of Arizona.

†Alfred P. Sloan Research Fellow.

‡Fannie and John Hertz Foundation Predoctoral Fellow.

[1]J. E. Mercereau, in *Superconductivity,* edited by R. D. Parks (Marcel Dekker, New York, 1969), Vol. I.

[2]R. W. Stark and L. M. Falicov, in *Progress in Low Temperature Physics,* edited by C. J. Gorter (North-Holland, Amsterdam, 1965), Vol. V, p. 235.

[3]L. Onsager, Phil. Mag. 43, 1006 (1952).

[4]A. V. Gold, in *Electrons in Metals, Simon Fraser Summer School Lectures, Solid State Physics, 1963,* edited by J. F. Cochran and R. R. Haering (Gordon and Breach, New York, 1968), Vol. I.

[5]J. C. Kimball, R. W. Stark, and F. M. Mueller, Phys. Rev. 162, 600 (1967).

[6]R. W. Stark, T. G. Eck, and W. L. Gordon, Phys. Rev. 133, A443 (1964).

[7]R. V. Kollarits, J. Trivisonno, and R. W. Stark, Phys. Rev. B 2, 1508 (1970).

[8]A. B. Pippard, Proc. Roy. Soc., Ser. A 287, 165 (1965).